



SCIREA Journal of Chemistry

<http://www.scirea.org/journal/Chemistry>

June 19, 2020

Volume 5, Issue 3, June 2020

Evaluation of antitumour potency of *Sonchus oleraceus* L. peptides on human gastric cancers *In vitro* and *In vivo*

Jie Liu^{a,b,†}, Huailing Wang^{a,c,†}, Xiaowei Zeng^e, Xizhuo Sun^a, Zhendan He^c, *Liteng Yang^{a,*},
Shuqi Qiu^{d,*}, Lin Mei^{e,*}

Affiliation:

^a The Third Affiliated Hospital of Shenzhen University, Shenzhen University, Shenzhen, 518020, China.

^b School of Medicine, Shenzhen University, Shenzhen 518060, China.

^c College of Pharmacy, Shenzhen Technology University, Shenzhen 518118, China.

^d Longgang ENT Hospital & Shenzhen ENT Institute, Shenzhen, 518060, China.

^e Graduate School at Shenzhen, Tsinghua University, Shenzhen 518055, China.

Corresponding authors:

Shuqi Qiu Telephone: (+86) 0755-86671937 E-mail: ssongyannan@sina.com

Liteng Yang Telephone: (+86) 0755-86671911 E-mail: songyannan@tom.com

Lin Mei Telephone: (+86) 0755-86671902 E-mail: songyannan@tom.com

†: Contributed equally to this work.

Abstract

The *Sonchus oleraceus* L. is widely consumed as vegetables, tea drink and traditional medicine. However, the anti-tumor property of *Sonchus oleraceus* L peptides (SOPs) was rarely explored. The present study evaluated the anti-gastric cancer potency of SOPs *in vivo*. We found that SOP-1 (FKEHGY) significantly inhibited the proliferation of the SGC-7901 cells with an IC_{50} of 0.10 ± 0.01 mM (24 h), and inhibited the growth of the gastric tumor in the experimental mice. Further study revealed that SOP-1 blocked the cell cycle in G0/G1 phase, and accompanied with inhibiting the cyclins expression of the gastric cancer cells collected from the tumor tissue of the SOP-1 treated mice. In addition, SOP-1 significantly increased the Bax/Bcl-2 ratio and induced the mitochondrial membrane potential collapse, and activated Caspases, thereby inducing the gastric cancer cells apoptosis. The current findings reveal that SOP-1 is a potent cytotoxic agent against gastric cancer cells *in vivo* and its cytotoxicity is mediated through induction of apoptosis and cell cycle arrest.

Keywords: *Sonchus oleraceus* L.; Gastric cancer; Cell cycle arrest, Apoptosis

1 Introduction

Gastric cancer is one of the most commonly diagnosed cancer, which is also the leading cause of cancer-related death worldwide. Gastric cancer can be further classified according to the disease site, which includes gastric cardia cancer, gastric cancer, and gastric antrum cancer[1]. It was estimated that nearly 700,000 people die from it and approximately 1,000,000 new patients are diagnosed worldwide each year, and the gastric cancer is one of the most common malignancies in the world and characterized by its high mortality rate[2]. In spite of great attention has been paid on the treatment of gastric cancer and a great improvement has emerged in the treatment of this disease, the median survival time for patients with this disease is still only 6-9 months. Gastric cancer is the most common malignant tumor in China, with the high-risk age of the disease is above 50 years old. In the past few decades, due to the

increase of pressure in daily life, and *Helicobacter pylori* infections, gastric cancer has been observed to have an earlier onset[3, 4].

Gastric cancer treatment involves chemotherapy with cisplatin alone or in combination with other chemotherapeutic agents. Combination chemotherapy with cisplatin as first- or second-line treatment for advanced and persistent gastric tumor have yielded decent responses and this treatment modality is well accepted[5]. One of the important criteria for potential anticancer drugs is the ability to selectively kill tumor, without harming normal cells. However, chemotherapy, which induces tumor cell cytotoxicity and eventually death, has not significantly improved the overall survival of patients with gastric cancer because of poor selectivity and toxicity[6]. Therefore, it is urgent and necessary to find novel anticancer agents with potent activity and high therapeutic index to improve current treatment of gastric cancer patients.

The traditional Chinese medicine (TCM) displayed an significant role in the prevention and treatment of tumors due to the advantage of proven safety. According to the previous reports, most of the agents approved by the Food and Drug Administration for cancer were extracted from traditional medicine or natural sources[7]. More recent attractions have been paid to the traditional Chinese medicine due to the advantage of proven safety in the prevention and treatment of cancer. *Sonchus oleraceus* L. has a widespread world distribution. It is edible to humans as a leaf vegetable and is frequently consumed in Australia, New Zealand, and particularly by the Chinese people[8]. In traditional Chinese medicine, aerial parts of *Sonchus oleraceus*, are used mostly in tea, and is administered orally for treating stomachic pain, hepatitis, infections, inflammation, headaches, general pain, rheumatism and toothaches. Of interest, in Italy, *Sonchus oleraceus* is used as a depurative and laxative and to facilitate hepatic and intestinal function. In Pakistan, the roots and leaves are used as a febrifuge, diuretic, laxative and general tonic[9]. The plant contains sorts of flavonoid glycosides, moreover, the alkaloids, coumarins, flavonoids and saponins have also been detected[10, 11]. In addition, antioxidant properties of the *Sonchus oleraceus* extract have previously been reported[12]. However, the effects of *Sonchus oleraceus* on protein expression in gastric cancer cells and the underlying mechanism of action are unclear. In current study, we

explored the anti-tumor effects of *Sonchus oleraceus* peptides against gastric cancer *in vivo*. Preliminary experiments showed that the peptide (SOP-1~FKEHGY) isolated from the *Sonchus oleraceus* can significantly inhibit the growth of the gastric tumor in the experimental mice, and induced the tumor cells apoptosis significantly, meanwhile, the potential molecular mechanism was also explored.

2. Methods

2.1 Isolation and amino acid sequence analysis of SOPs

The *Sonchus oleraceus* L. was acquired from the Ertiantang Pharmacy (Guangzhou, China) and identified by Professor Zhou (South China Agricultural University, Guangzhou, China). The *Sonchus oleraceus* L. was minced and defatted. Briefly, the homogenate and iso-propanol were mixed in a ratio of 1:10 (w/v) and stirred uninterrupted for 5 h at 0°C. The iso-propanol was replaced every 30 min. All extraction and separation procedures were performed at 4°C. The supernatant was removed, and the sediment was freeze-dried and stored at -20°C as the total *Sonchus oleraceus* L. protein. The total *Sonchus oleraceus* L. protein was fractionated using ultrafiltration with 1 kDa molecular weight (MW) cut off membranes (Millipore, Hangzhou, China) for the lab scale. Two peptide fractions, called SOP-A (MW < 1 kDa) and SOP-B (MW > 1 kDa), were collected and freeze-dried.

Then, the total SOP-A fraction (50.5 g) was homogenized in 600 mL of 10 mM ammonium acetate (pH 6.4) using Potter-Elvehjam homogenizer and the insoluble material was removed by centrifugation at 15,000 rpm for 30 min[13]. An additional 100 mL of ammonium acetate was added to the pellet, the homogenization was repeated, the contents were centrifuged and the supernatant was collected. The above procedure was repeated 5 times to maximize the yield of peptides from the venom.

The supernatant fractions were pooled, passed through a pre-cycled CM-52 column and eluted with a gradient of 0.01 M to 0.60 M ammonium acetate (pH 6.4) at a flow rate of 10 mL/h. Fractions (80 mL), were collected using a BioRad (Model 2110) fraction collector. All the chromatographic separations were carried out at 4°C. Individual fractions were monitored at

280 nm using a Shimadzu spectrophotometer (UV-3101). Chromatographic analysis was done by HPLC (Thermo Fisher Scientific, UltiMate 3000 RS LC nano). The UV measurements were performed simultaneously at 230 and 300 nm. A 6 μm particle size Protein C4 column (25 cm \times 9.4 mm, Agilent Zorbax, GF250) was used. The column was maintained at 20°C. Chromatographic peaks were integrated and the freeze dried fractions were resuspended in water and aliquots of 1 mg each were loaded onto the C4 reversed phase column equilibrated in Solvent A (A = 5% methanol, 0.1% trifluoroacetic acid, TFA). The individual peptides were eluted from the column with a linear gradient reaching 45% Solvent B (B = 95% methanol; 0.1% TFA) in a flow rate of 1.0 mL/min. All the fractions were collected, freeze dried and assayed for anti-gastric cancer activity. The active fractions were further purified using a Protein C4 Column (25 cm \times 4.6 mm, TSKgel Protein C4-300) equilibrated with Solvent A (A = 5% methanol; 0.1% heptafluorobutyric acid (HFBA) and resolution of peaks was accomplished using gradient elution of solvent B (B = 95% methanol; 0.1% HFBA) reaching 50% in a flow rate of 1.0 mL/min. Individual peaks were collected and lyophilized, following two HPLC steps, the peptides were further purified using a C18 reversed-phase column (Michrom 10 cm \times 1 mm) on a Microbore HPLC system (Michrom Bioresources Inc., USA). The peptides were loaded onto the C18 column and eluted in a linear gradient of 30-70 % Solvent B (95% methanol; 0.1% TFA) over 100 min at a flow rate of 1.0 mL/min.

HPLC-ESI-MS was performed on a SCIEX X500R Q-TOF mass spectrometer (Framingham, U.S.A.). And the MS conditions were set as follows: ESI-MS analysis was performed using a SCIEX X500R Q-TOF mass spectrometer equipped with an ESI source. The mass range was set at m/z 100-1500. The Q-TOF MS data were acquired in positive mode and conditions of MS analysis were as follows: CAD gas flow-rate, 7 L/min; drying gas temperature, 550°C; Ion spray voltage, 5500 V; Declustering potential, 80 V. Software generated data file: SCIEX OS 1.0[14].

Further, the purity of the SOPs (> 97.0%) was determined by HPLC.

2.2 Cell culture and cell counting *cit-8* (CCK-8) assay

Human gastric cancer cell lines in current study were obtained from Keygen Biology Co., Ltd., (Nanjing, Jiangsu, China). The cells were cultured with RPMI 1640 medium (Gibco,

Rockville) containing 10% fetal calf serum (Gibco, Invitrogen, MD, USA), 0.1 µg/L penicillin, and 0.1 µg/L streptomycin (P1400, Solarbio, Beijing, China) and were incubated in a 5% CO₂ incubator at 37°C.

The effect of SOPs on the viability of the gastric cancer cells was determined using a CCK-8 assay[15]. Gastric cancer cells were cultured in the medium and, upon reaching the logarithmic growth phase, were digested with 0.25% trypsin + 0.02% ethylene diamine tetraacetic acid (EDTA), centrifuged at 600×g for 3 min, and collected. After counting, 100 µL of the cell suspension was seeded in each well of a 96-well plate at a density of 1.2×10^5 cells/mL. After 24 h of culture, culture medium containing 0.1-4.0 mM of SOPs were added and further cultured for another 24 h in the incubator. After 24 of culture, 10 µL of CCK-8 solution was added to each well and incubated for 4 h. Then, the plate was shaken for 1 min in the dark, and the absorbance of each well at a wavelength of 450 nm was detected using a microplate reader (Bio-Rad; Hercules, CA, USA). The absorbance of the cells treated with 0.1% DMSO in RPMI 1640 was used as a control (survival rate: 100%). IC₅₀ (half maximal inhibitory concentration) indicates a drug concentration resulting in a 50% reduction in cell survival.

The anti-colony formation of tumor cells potency of the SOP-1 was evaluated as follows: Briefly, SGC-7901 cells were plated in 6-well plates with 4000 cells per well in 4 mL complete medium (RPMI1640 medium supplemented with 10% fetal bovine serum, 100 U/mL penicillin, 0.1 mg/mL streptomycin and 2 mM L-glutamine). After 48 h, the wells were added the SOP-1 . The complete culture medium was replaced every three days, and the culture was terminated until the cell community visible to the naked eye appeared in the six-pore plate in two weeks. 1 mL PBS was added to the well and washed three times, then, 1 mL methanol was added to each well and fixed for 15 min. After that, the methanol was discarded, and 1 mL Gemsa dye solution was added and cultured for 15 min.

2.3 Xenograft model of gastric neoplasm

The animal study procedures were approved by the Animal Ethic Committee at Shenzhen University. Mice were maintained in a specific pathogen-free facility followed the standard specific pathogen-free breeding protocol. There were 30 nude mice with a mean weight of 20

± 2 g, and the ratio of male to female was 1:1. A number of 1×10^6 SGC-7901 cells was i.p. injected into the mice. Tumor growth was measured every 2 days. When tumor volume reached 0.25 cm^3 , the mice were randomly divided into three groups and treated with the following procedures: **Control**: the mice were injected with 200 μL saline every 4 days around the tumor tissue; **SOP-1-L**: mice were injected with SOP-1 (in 200 μL saline) 0.5 mg/kg every 4 days (4 days a cycle, four times) around the tumor tissue; **SOP-1-H**: mice were injected with SOP-1 (in 200 μL saline) 2.5 mg/kg every 4 days (4 days a cycle, four times) around the tumor tissue. Then all mice were sacrificed on day 23. Subcutaneous tumors were excised and the tumor index was calculated. In addition, the tumor tissue were cut into small woven pieces and fixed with polyformaldehyde, and the paraffin sections were made later. The tumor inhibition rate was calculated according to the following formula.

Tumor inhibition rate (%) = (The average tumor weight in control group - the average tumor weight in experimental group) / the average tumor weight in control group.

2.4 Tumor apoptosis assessment and HE staining

The apoptotic cells in the gastric cancer tissue sections were stained with a TUNEL reagent kit following the manufacturer's instructions. HE staining was performed according to the routine procedure. Paraffin section was dewaxed and dehydrated by xylene and gradient alcohol, then stained with hematoxylin solution for 5 min, then soaked in 1% acid ethanol (1% HCl in 70% ethanol) for 2 min, and rinsed in distilled water. The slices were stained with eosin solution for 3 min, dehydrated with graded alcohol and cleaned with xylene.

The cell cycle distribution was determined by flow cytometry[16]. Briefly, after the mice were sacrificed, the tumor cells were collected, washed with cold PBS, then the cells were fixed overnight in 70% ethanol at 4°C . After fixation, the cells were centrifuged at $3000 \times g$ for 5 min to remove the ethanol. Then, the cells were washed with PBS, treated with 100 μL of RNase A, resuspended, and incubated at 37°C for 30 min in the dark. Fluorescence detection of propidium iodide (PI)-DNA complexes was determined by flow cytometry (BD FACS Calibur, Franklin Lakes, CA, USA). All the tests were repeated at least 3 times.

Further, the apoptosis of the gastric cancer cells collected from the tissue of the experimental

mice were also evaluated by the flow cytometry. The Annexin V-FITC/PI double staining assay was performed according to the manufacturer's instructions[17]. Briefly, after the mice were sacrificed, the tumor cells were collected, washed, and were resuspended in precooled $1 \times$ PBS and centrifuged at $2000 \times g$ for 3 min, and the cells were washed. The cells were resuspended by adding 500 μ L of $1 \times$ binding buffer. Then, 5 μ L of Annexin V-FITC was added to the suspension, mixed well, and incubated for 15 min at room temperature. The cells were then stained with 5 μ L of a PI staining solution before loading into a flow cytometer (BD FACS Calibur, Franklin Lakes, CA, USA). All the tests were repeated at least 3 times.

2.5 Mitochondrial membrane potential assay and western blotting analysis

The JC-1 method was used to evaluate the mitochondrial membrane potential, and performed according to the manufacturer's instructions[18]. The tumor cells were collected from the gastric cancer tissue after the SOP-1 treatments as the experimental design, washed twice with PBS, and incubated with JC-1 working solution for 0.5 h at $37^{\circ}C$ without light. After incubation, the cells were collected and centrifuged at $2000 \times g$ for 3 min at room temperature. The cells were resuspended in prechilled $1 \times$ JC-1 staining buffer, centrifuged at $2000 \times g$ for 3 min, and washed twice. The cells were resuspended by the addition of 500 μ L of JC-1 staining buffer and then loaded onto a flow cytometer (BD FACS Calibur, Franklin Lakes, CA, USA).

The tumor cells were collected from the gastric cancer tissue after the SOP-1 treatments as the experimental design, washed with PBS, lysed in the lysis buffer containing protease and phosphatase inhibitor cocktails and centrifuged at $1.3 \times 10^4 g$ for 12 min. Immunoblotting assay was performed as described and with brief modifications. Proteins from cell supernatants were then charged on a 15 % dodecyl sulfate polyacrylamide running gel. After the electrophoresis run, proteins were transferred from the gel to nitrocellulose membranes, using a Trans-Blot Turbo Transfer System and then membranes were blocked with TBS-T containing 5 % non-fat milk for 1 h. Membranes were incubated at $4^{\circ}C$ overnight with the primary antibody solution, diluted at 1:500 (v/v). Then membranes were probed for 1 h at room temperature with their specific alkaline phosphatase conjugated secondary antibodies ($1:8 \times 10^3$ dilution v/v). The protein bands were measured and the β -actin was used as an internal standard of process control[19]. Blot bands densitometry was analyzed with Image *J*

software.

2.6 Statistical Analysis

The data are presented as the mean± standard deviation (SD). GraphPad Prism 5.0 (Graph Pad Software, La Jolla, CA, USA) was used for statistical analysis. Statistical analysis was performed with one-way analysis of variance (ANOVA). $p < 0.05$ was considered statistically significant.

3 Results and Discussion

3.1 *In vitro* anti-gastric cancer potency of SOPs

The peptide is usually protonated under ESI-MS/MS conditions, and fragmentations mostly occur at the amide bonds because it is difficult to break the chemical bonds of the side chains at such low energy. Therefore, the b and y ions are the main fragment ions when the collision energy is < 200 eV[20]. The SOP-1 was analyzed by HPLC-ESI-MS for molecular mass determination and peptide characterization (**Figure 1**).

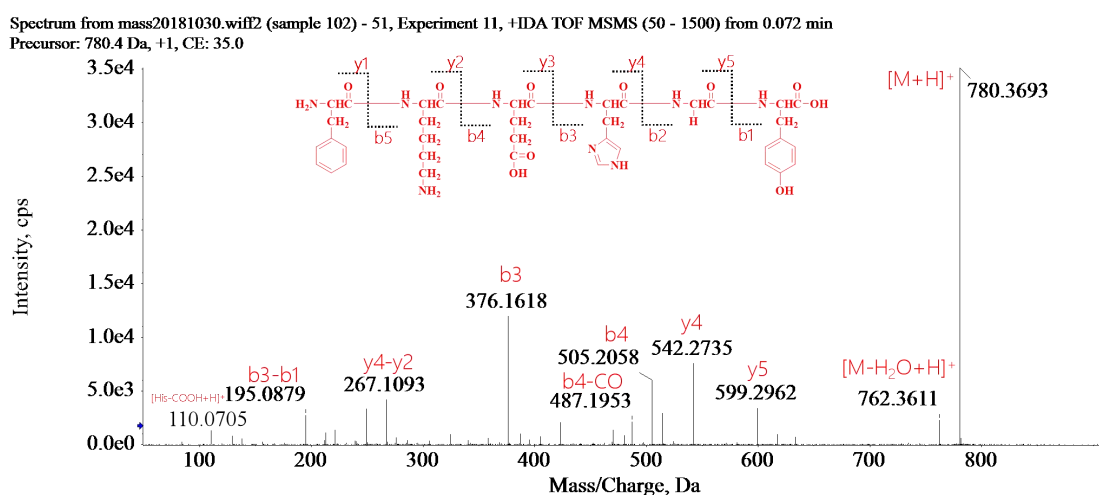


Figure 1 MS spectrum and structure of SOP-1

The ion fragment m/z 780.3693 was regarded as $[M+H]^+$. The ion m/z 762.3611 was regarded as the $[M-H_2O+H]^+$ fragment, while m/z 599.2962 was regarded as the y5 ion, m/z 542.2735 was regarded as the y4 ion and m/z 505.2058 was regarded as the b4 ion, m/z 487.1953 was regarded as the $[y4-CO]^+$ fragment. The ion (m/z 376.1618) was the b3 ion, and ion (m/z

267.1093) was the y4-y2 ion, m/z 195.0879 was the b3-b1 ion, m/z 110.0705 was the [His-COOH+H]⁺ fragment. On the basis of this, we concluded that the sequence of the peptide was FKEHGY. The rest of the SOPs were identified as SOP-1, and the amino acid sequences are list in **Table 1**. Finally, sixteen novel SOPs were isolated and their amino acid sequences were identified. Further, the purity was detected by HPLC > 97.0%.

Table 1 Inhibition of proliferation in gastric cancer cells of SOPs

SOPs	Amino Acid Sequence	IC ₅₀ (mM)		
		SGC-7901	MKN-45	MGC-803
SOP-1	FKEHGY	0.10 ± 0.01	0.15 ± 0.02	0.21 ± 0.03
SOP-2	FEFHL	2.25 ± 0.22	1.71 ± 0.13	0.62 ± 0.05
SOP-3	EGFHL	1.42 ± 0.12	> 4.0	1.70 ± 0.15
SOP-4	EHGEYE	0.56 ± 0.03	0.74 ± 0.08	0.72 ± 0.08
SOP-5	FRHALS	1.12 ± 0.10	1.05 ± 0.11	0.88 ± 0.06
SOP-6	EGHGF	1.04 ± 0.12	1.32 ± 0.13	1.46 ± 0.13
SOP-7	WEHKHA	> 4.0	1.76 ± 0.14	> 4.0
SOP-8	LWEHSH	1.13 ± 0.14	1.66 ± 0.11	1.44 ± 0.12
SOP-9	KYGHEHS	2.84 ± 0.24	3.63 ± 0.25	> 4.0
SOP-10	YSHMYR	1.11 ± 0.12	1.34 ± 0.14	> 4.0
SOP-11	WLHMWP	1.23 ± 0.12	1.32 ± 0.12	1.58 ± 0.16
SOP-12	HKYNWP	1.27 ± 0.14	1.21 ± 0.11	1.41 ± 0.15
SOP-13	HSYAWKP	2.21 ± 0.25	2.19 ± 0.19	2.46 ± 0.25
SOP-14	WTHDWKR	0.23 ± 0.04	0.36 ± 0.03	0.44 ± 0.05
SOP-15	YEHCYR	1.81 ± 0.17	2.13 ± 0.22	3.01 ± 0.26
SOP-16	WGHIYP	1.53 ± 0.14	1.71 ± 0.19	2.46 ± 0.22

IC₅₀ values are shown as mean ± standard error of the mean (SD), from at least three independent experiments. The three cancer cell lines were seeded into 96-well plates, and cells were treated with different concentrations of SOPs for 24 h. The survival rate of cells treated with SOPs was measured by the CCK-8 method.

Currently, chemotherapy is a mainly approach for the treatment of gastric cancer, and drug resistance is one of the most significant obstacles in chemotherapy. Besides, toxicities of using high doses of chemotherapeutic agents to get over drug resistance also significantly impede patients' recovery[21]. Therefore, it is urgent and necessary to find novel anticancer agents with potent activity and high therapeutic index to improve current treatment of gastric cancer patients. The traditional Chinese medicine (TCM) displayed an significant role in the prevention and treatment of tumors due to the advantage of proven safety[22]. To study the effect of SOPs on gastric cancer *in vitro*, we treated the three gastric cancer cell lines (SGC-7901, MKN-45 and MGC-803) with different concentrations of SOPs for 24 h. The activity of the cancer cells after SOPs treatment was detected by the CCK-8 assay.

As shown in **Table 1**, most of the SOPs performed anti-proliferative activity against the three human gastric cancer cell lines. Interestingly, SOP-1 potently inhibited the growth of SGC-7901, MKN-45 and MGC-803 cells, with IC₅₀ values of 0.10 ± 0.01, 0.15 ± 0.02, 0.21 ± 0.03 mM, respectively. Since SOP-1 was indicated enhancing the anti-proliferative activity in SGC-7901 cancer cells, together with the fact that gastric cancer is one of the most common malignancies. This is the reason why we performed further experiment *in vivo* to explore the anti-cancer potency of SOP-1.

In current experiment, the cytotoxicity of the SOP-1 in normal cells from healthy tissue was also evaluated. The cytotoxicity of SOP-1 in human gastric epithelial cells (GES-1) and human liver cells (HL-7702) are at much higher levels compared with the tumor cells, in which the IC₅₀ values are 3.43 ± 0.22 mM to GES-1 and 3.76 ± 0.29 mM to HL-7702.

3.2 SOP-1 inhibits tumor cell colony formation *in vitro*

The colony number of more than 50 cells, and 36 visual fields were respectively counted under an optical microscope for statistical analysis (**Figure 2A**). Statistical analysis showed

that SOP-1 significantly inhibited the formation of the tumor cell colony. After calculation, the colony forming rate of blank group was 17.3% (colony forming rate (%) = (number of colonies / number of concentrated cells) × 100%), that of SOP-1-L group was 23.2%, that of SOP-1-H group was 31.6%.

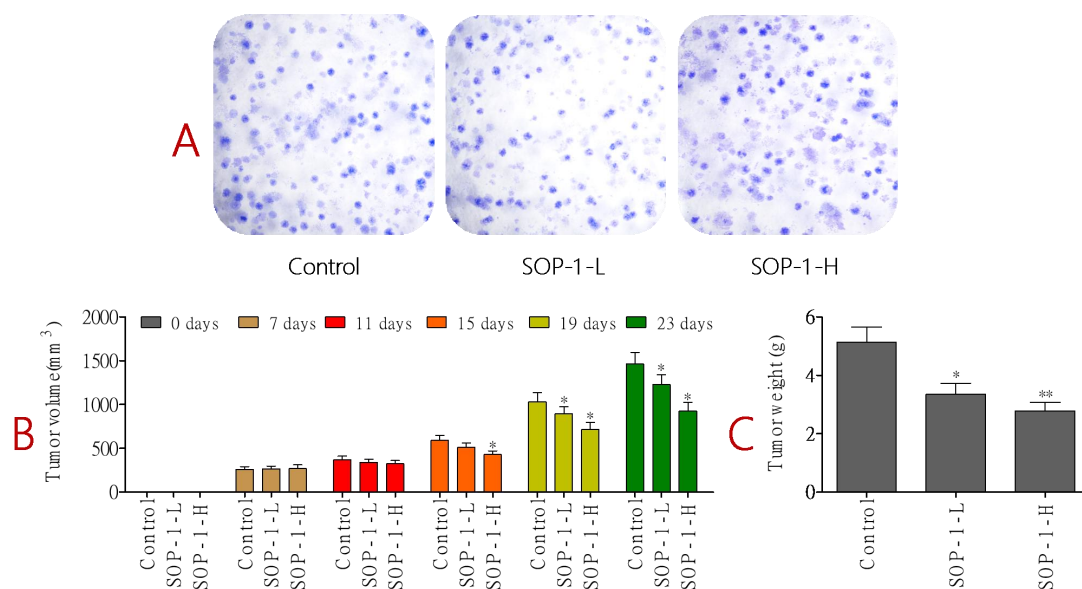


Figure 2 SOP-1 inhibited the tumor cell colony formation and the tumor growth

(A) SGC-7901 cells were cultured with six well plates, 4000 cells/well. After stabilization, the SOP-1 were added to the culture. The culture medium was changed every 3 days until 6 pore plates showed visible cell colonies. (B) Representative images of the formation of cell colonies. Mice were subcutaneously injected with SGC-7901 cells (10^6 cells/mouse) into the side of the back skin near the armpit. One week later, mice were divided into three groups and injected with SOP-1 or saline (control), around and inside the tumor tissues weekly for three weeks. Bars showed the changes of tumor size and weight. (C) After the mice were sacrificed, the tumor were weighed.

3.2 SOP-1 slows down the growth of the gastric tumor in the experimental mice

One week after inoculation, the mice were grouped and treated with saline or SOP-1 for 3 weeks. To evaluate tumor growth in mice, the tumor volume was calculated and tumor weight was recorded after the sacrifice, and the results were shown in **Table 2** and **Figure 2B** and **2C**. On day 15, the tumor volume in the control group increased by 1.27%; the tumor volume in the SOP-1-H group increased by 59.3%, which indicated that the SOP-1 inhibited the tumor

growth significantly. Further, on day 23, the tumor volume in the control group increased by 461%; the tumor volume in the SOP-1-H group increased by 240%. The SOP-1 definitely inhibited the tumor growth.

Of interest, the SOP-1 treatments also attenuated the weight up-regulation of the gastric tumor in the mice. Compared to the control group (the tumor weight was set as increases by 100%), the tumor inhibition rate of SOP-1 treatment was 34.8% (SOP-1-L, $p < 0.05$), and 45.7% (SOP-1-H, $p < 0.01$), respectively (**Figure 2C**).

Table 2 Effect of peritumoral injection of SOP-1 on the tumor size

Tumor volume (cm³)	Day 0	Day 7	Day 11	Day 15	Day 19	Day 23
Control group	0	0.26±0.03	0.37±0.04	0.59±0.05	1.03±0.10	1.46±0.13
SOP-1-L	0	0.26±0.03	0.34±0.03	0.51±0.05	0.89±0.08	1.23±0.11
SOP-1-H	0	0.27±0.04	0.32±0.04	0.43±0.04	0.71±0.08	0.92±0.10

IC₅₀ values are shown as mean ±standard error of the mean (SD). Mice were subcutaneously injected with SGC-7901 cells (10⁶ cells/mouse) into the right side of the back skin near the armpit. One week later, mice were divided into three groups and injected with SOP-1 or saline (control), around and inside the tumor tissues weekly for three weeks. During 23 days of observation and treatments, no mice died.

3.3 SOP-1 induces gastric cancer cells apoptosis and necrosis in the mice

Cell apoptosis is a pivotal anticancer target with distinct morphological features, such as cytoplasmic shrinkage, membrane blebbing and chromatin condensation. The necrosis is a form of traumatic cell death that results from acute cellular injury; while apoptosis is a highly regulated and controlled process that confers advantages during an organism's life[23]. In current experiment, the gastric cancer tissue was stained by TUNEL staining.

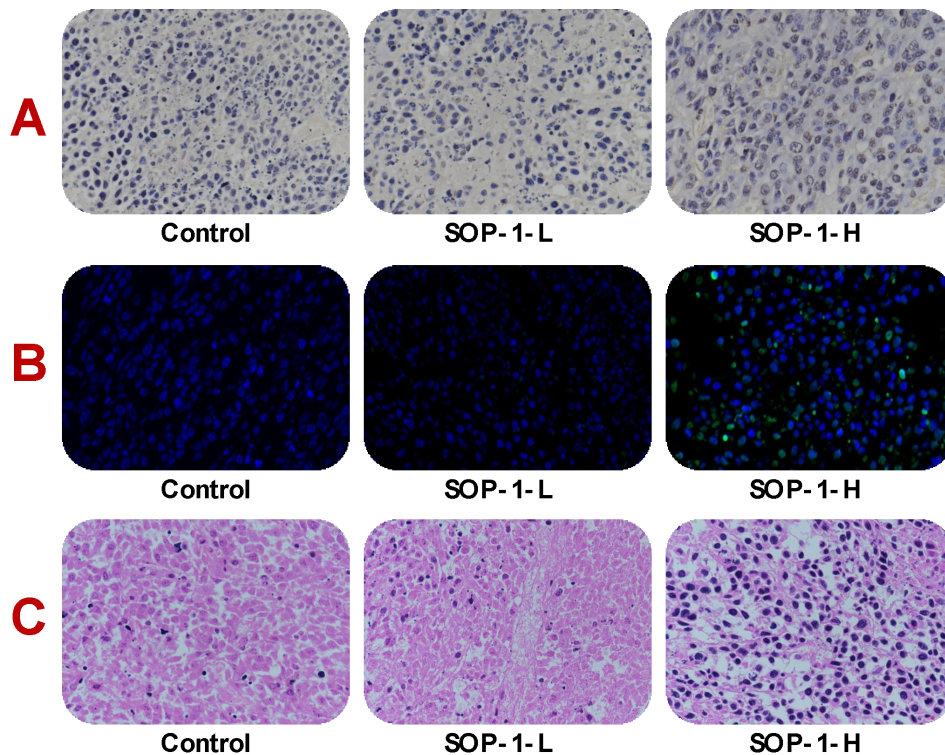


Figure 3 SOP-1 induces apoptosis and necrosis of gastric cancer cells in the mice

The tumor tissues were taken from the mice and fixed with formalin. The paraffin sections were prepared and stained with the appropriate procedures. **A** TUNEL ordinary staining, the TUNEL positive cells were stained in brown, and refers to the apoptosis of the cells; **B** TUNEL fluorescence staining, the TUNEL positive cells were stained in green; **C** HE staining, the paraffin sections were prepared and stained with HE, and shows the edema around the necrotic focus of tumor tissue.

The apoptotic cells were stained in brown, and the results were shown in **Figure 3A**. The apoptotic cells in SOP-1 groups were significantly increased than those in the control group. After TUNEL fluorescent staining, the apoptotic cells were stained to green as observed under the fluorescence microscope (**Figure 3B**). The number of apoptotic cells was counted in 6 visual fields of each group. The results showed that the SOP-1-L treatment significantly induced the cell apoptosis than those in the control group ($p < 0.05$). The results demonstrated that the SOP-1 injection can induce the gastric cancer cells apoptosis significantly.

The tumor tissue was taken and fixed with formalin, then the paraffin sections were prepared and stained with HE. The results showed that there were large necrosis cells in tumor tissue, pyknosis fragmentation and dissolution of nuclei. The necrosis area of tumor tissue in

SOP-1-L group was significantly larger than that in the control group; and the intercellular space between tissues widened significantly in SOP-1 group (**Figure 3C**).

3.4 SOP-1 promotes Caspase-dependent apoptosis in the gastric cancer cells

The apoptosis is a programmed cell suicide characterized by chromatin condensation, DNA fragmentation, cell shrinkage, membrane blebbing and apoptotic body formation. The process of apoptosis plays key role in the development of the cancers. Further, the tumors subjected to radiation and cytotoxic agents showed increased rates of apoptosis, implying that enhanced rate of apoptosis can be used in cancer therapy[24].

To explore whether the inhibition of the tumor growth potency of SOP-1 is related to the cell apoptosis, we analyzed the apoptotic rate of the gastric cancer cells in the SOP-1-treated mice using an Annexin V FITC/PI double staining kit and flow cytometry. We found that the percentage of apoptotic cells increased significantly after the SOP-1 treatments, from 3.42% (control) to 21.1% (SOP-1-L) and 33.9% (SOP-1-H), respectively (**Figure 4A**). These results indicated that SOP-1 effectively induced the cell apoptosis in the gastric cancer cells collected from the experimental mice.

The Caspase activation is considered to be a hallmark of apoptosis, we then checked whether the Caspase activation is involved in SOP-1 induced cell apoptosis. As shown in **Figure 4B**, both the Cleaved caspase-9 and Cleaved caspase-3 were increased in SOP-1-treated mice. Meanwhile, the Cleaved PARP was also strongly activated in the gastric cancer cells of SOP-1-H treated mice.

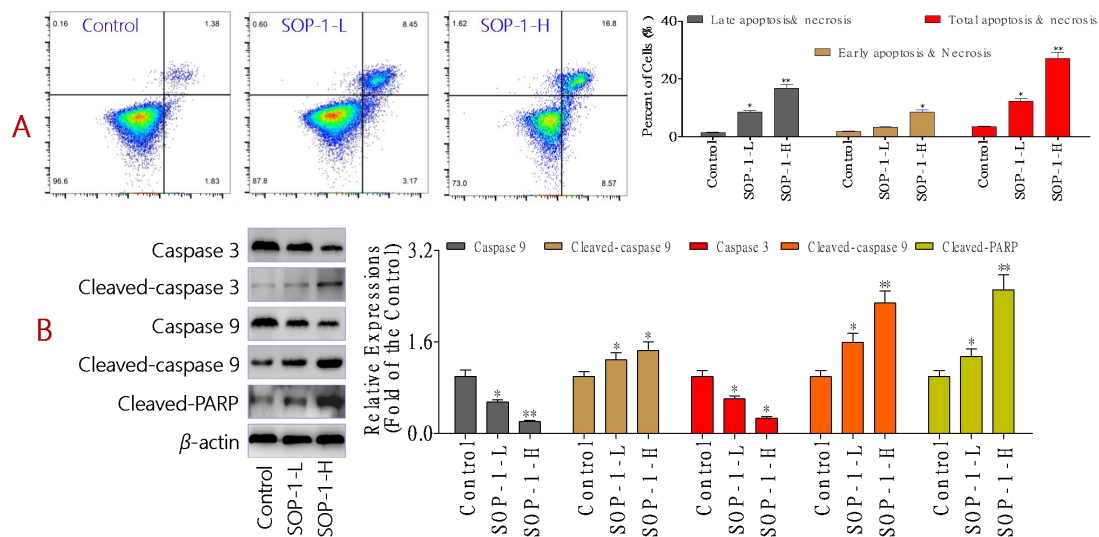


Figure 4 SOP-1 induces gastric cancer cells apoptosis

(A) Representative scatter diagrams. After the SOP-1 treatments, the gastric cancer cells were collected from the tumor tissue. After that, cell apoptosis was measured by flow cytometry. Flow cytometric analysis of cell apoptosis was evaluated by Annexin V-FITC/PI staining. Cells in the lower right quadrant (Annexin V⁺/PI⁻) represent early apoptotic cells, and those in the upper right quadrant (Annexin V⁺/PI⁺) represent late apoptotic cells. (B) SOP-1 activates Caspase cleavage in the gastric cancer cells. After the SOP-1 treatments, the cells were collected from the tumor tissue. The Cleaved-PARP, Caspase 3, Cleaved-caspase 3, Caspase 9 and Cleaved-caspase 9 expressions were detected by Western blotting. β -actin was used as an internal control. The data are expressed as the mean \pm SD of 3 independent experiments. * $p < 0.05$, ** $p < 0.01$, compared with the control group.

3.5 SOP-1 arrests the cell cycle of the gastric cancer cells in G0/G1 phase by regulating the cyclins expression

Checkpoints are important regulatory nodes of the cell cycle, and cells can only enter the next cell cycle after passing these checkpoints[25]. The function of the G0/G1 phase detection point is to integrate and transmit complex intracellular and extracellular signals, such as various growth factors, mitogens, and DNA damage, as well as to determine whether cells are undergoing division and apoptosis. Deregulation of cell cycle progression is a common feature of cancer cells. Therefore, targeting the regulatory cyclins has been proposed as an important strategy for the treatment of human malignancies[26].

To further investigate the inhibitory effect of SOP-1 on the growth of the gastric tumor in the experimental mice, we examined the cell cycle distribution of the tumor cells after the treatments of SOP-1, and the results were shown in **Figure 5A**. Compared to the control group, flow cytometry analysis showed that the proportion of the tumor cells in G0/G1 phase was significantly increased after treatment with SOP-1. Briefly, the percentage of cells in G0/G1 phase increased from 38.0% (Control) to 53.7% (SOP-1-L) and 60.7% (SOP-1-H), respectively.

When the cells begin to synthesize DNA during G1/S conversion, CDK2 will combine with its regulatory subunit cyclin E to form a CDK2/Cyclin E complex, leading to Rb phosphorylation, and then E2F factor is released and cells are accelerated into the S phase[27]. So, we examined the cyclins expression of CDK2 and 6, cyclin D and E in the tumor cells after the SOP-1 treatment, and the results were shown in **Figure 5B**. Of interest, the expressions of cyclin D, cyclin E, CDK2 and CDK6 were all attenuated after the SOP-1 treatments, which suggested that SOP-1 induced cell cycle arrest in G0/G1 phase may be by inhibiting the expression of the cyclins.

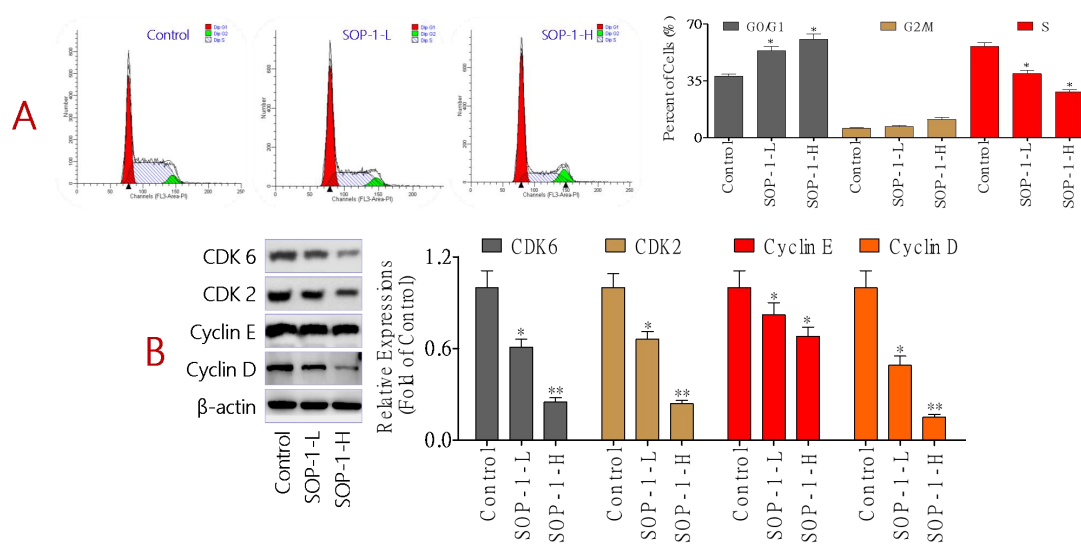


Figure 5 SOP-1 induces G0/G1 cell cycle arrest of the gastric cancer cells by inhibiting the cyclins expression

After the SOP-1 treatments, the gastric cancer cells were collected from the tumor tissue. (A) Flow cytometry was used to determine the cell cycle distribution of the gastric cancer cells; (B) Western blotting

was performed to detect cyclin D, cyclin E, CDK2 and CDK6 expressions. β -actin was used as a loading control. The ratio of protein levels was normalized according to the values of the control. All data are expressed as the mean \pm SD of three independent experiments. * p < 0.05, ** p < 0.01 compared to the control.

3.6 SOP-1 blocked the cell cycle of the gastric cancer cells by regulating the protein expression of the ATM/p21 signaling pathway

The cell cycle refers to the entire process of continuous cell division. When cell cycle arrest occurs during cell division, it is often due to damage or errors that are difficult to repair during cell division. This theory suggests that SOP-1-induced G0/G1 arrest may be due to DNA damage that is difficult to repair in cells. The ATM/ATR signaling pathway can repair damaged DNA by modulating the activity of various proteins. At present, it is generally believed that the ATM/ATR signaling pathway mediates G0/G1 arrest by regulating the expression of p53[28]. ATM can directly regulate p53, which increases the p53 protein level, which in turn enhances p21 transcription. Activation of ATM during DNA damage can upregulate the expression of the p21 protein and down-regulate p53 protein expression. Finally, the formation of the CDK2/cyclin E complexes is inhibited, and the cell cycle is arrested at the G0/G1 phase[29]. The p21 is potent cyclin-dependent kinase inhibitors that bind to and inhibit the activities of CDKs; thus, increased expressions of these proteins thus indicate the induction of G0/G1 cell cycle arrest. Therefore, we detected whether the SOP-1 up-regulate the p53 expressions. Further, the protein expressions of ATM and p21 in the gastric cancer cells after the SOP-1 treatment were also evaluated by western blotting.

To our expect, the p21 and ATM expressions were up-regulated in the gastric cancer cells after the SOP-1 treatments, indicating that SOP-1 is related to p21-dependent cell cycle arrest. Further, SOP-1 up-regulated p53 expression (**Figure 6A**).

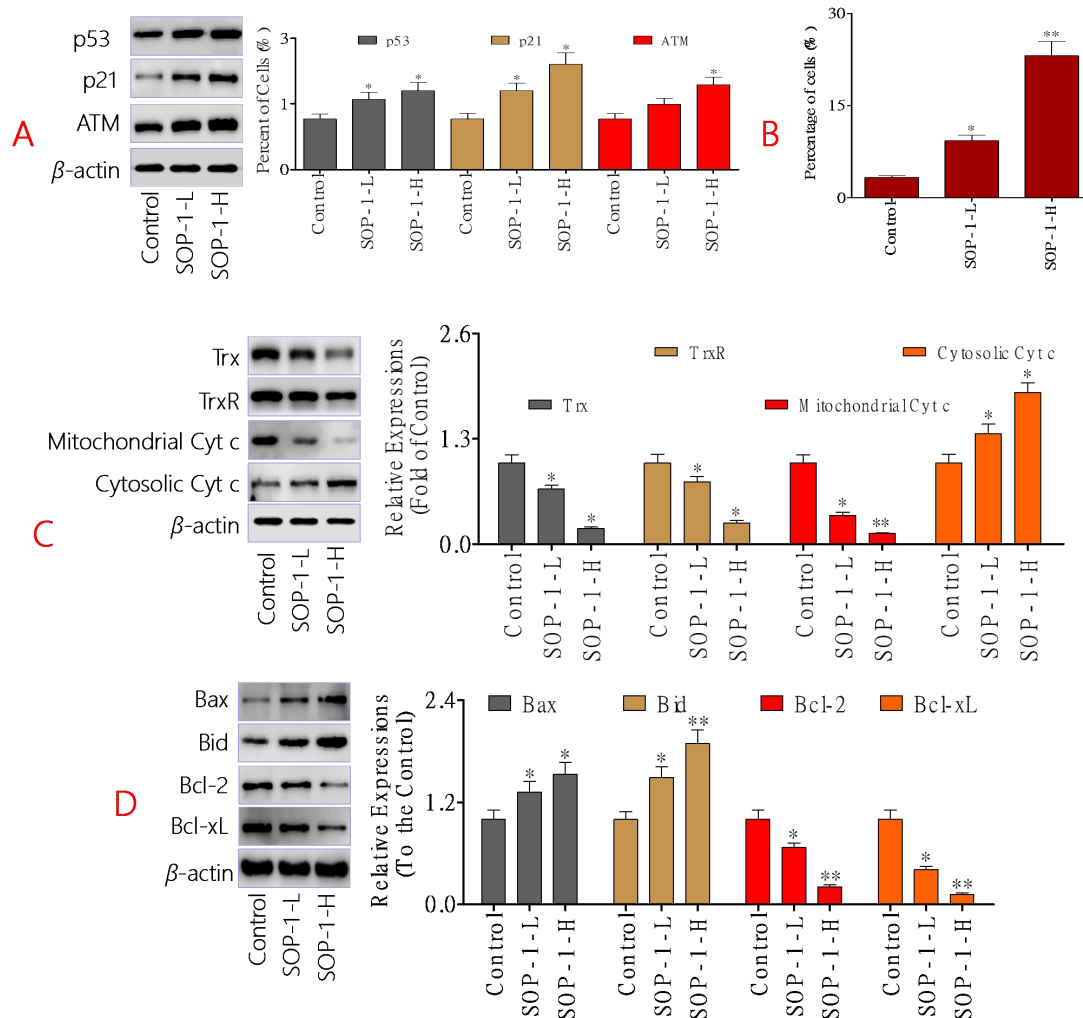


Figure 6 SOP-1 regulated the protein expressions in the ATM/P21 and the mitochondrial apoptotic pathways

After the SOP-1 treatments, the gastric cancer cells were collected from the tumor tissue. (A) Western blotting was performed to detect the p53, p21 and ATM expressions; (B) The decline of $\Delta\psi_m$ in the gastric cancer cells was detected by JC-1 staining and assayed by flow cytometry (BD FACS Calibur, Franklin Lakes, CA, USA); (C) Western blotting was performed to detect the expressions of Trx, TrxR, cytosolic and mitochondrial levels of the pro-apoptotic proteins cytochrome c; (D) Western blotting was performed to detect the levels of Bcl-2, Bcl-xL, Bid and Bax. The ratio of protein levels was normalized according to the values of the control. All data are expressed as the mean \pm SD of three independent experiments. * $p < 0.05$, ** $p < 0.01$ compared to the control.

3.7 SOP-1 induces apoptosis through mitochondrial pathways

The balance of $\Delta\psi_m$ and mitochondrial integrity is significant for the physiological function

of cells. Previous studies reported that collapse of $\Delta\psi_m$ was correlated to the events of apoptotic process. When the concentration of ROS and oxidative stress reach a certain level, the $\Delta\psi_m$ would be changed, resulting in the release of apoptosis factors[30]. In current study, the JC-1 fluorescent probe was used to detect the potency of SOP-1 on $\Delta\psi_m$ of the gastric cancer cells. As shown in **Figure 6B**, the SOP-1 treatments induced a clearly $\Delta\psi_m$ decrease signal. Compared to the control group, the cells suffered the $\Delta\psi_m$ decrease increased by 5.59%, and 12.8%, respectively, after the SOP-1 treatments.

The thioredoxin (Trx) system plays a critical role in the regulation of cellular reduction-oxidation (redox) homeostasis, further, over-expression of Trx and TrxR were found in most of cancer cells[31]. As shown in **Figure 6C**, the both the Trx and TrxR expressions were down-regulated, after the SOP-1 treatments, suggesting that this effect may be part of the mechanism of action for SOP-1.

The mitochondrion-dependent pathway is the most common apoptotic pathway in vertebrate tumor cells[32]. Mitochondrial dysfunction, as indicated by the dissipation of $\Delta\Psi_m$, could subsequently cause the release of cytochrome c (Cyt c) from mitochondria into the cytosol. Cytochrome C in the cytoplasm activates Apaf-1 and caspase-9 and -3, which cleaves DNA and produces apoptotic bodies that ultimately lead to apoptosis[33]. In the above experiments, we observed that SOP-1 could effectively induce apoptosis of the gastric cancer cells accompanied with the Caspases activation. So, we further examined the expressions of the aforementioned proteins in the mitochondrial apoptotic signaling pathway.

The results showed that SOP-1 treatments induced a striking up-regulation of cytosolic Cyt c and down-regulation of mitochondrial Cyt c (**Figure 6C**). Further, we investigated the expressions of the Bcl-2 family of apoptosis regulator proteins. We found that SOP-1 significantly increased the expressions of Bad and Bax and decreased the expressions of Bcl-2 and Bcl-xL, relative to the control group (**Figure 6D**).

4 Conclusion

Of note, we demonstrated that SOP-1 (FKEHGY) isolated from *Sonchus oleraceus* L. has a

growth-inhibitory potency on gastric tumor *in vivo*. We revealed that SOP-1 induces the gastric cancer cell apoptosis through the Caspase-dependent mitochondrial pathway and via G0/G1 phase block by regulating the expression of the cyclins. We also found that SOP-1 significantly down-regulated the ratio of Bax/Bcl-2, and activated the mitochondrion-dependent pathway.

Acknowledgments

We thank Professor Chen for technical assistance as well as critical editing of the manuscript. We thank Professor Chen for technical assistance as well as critical editing of the manuscript. The present study was supported by grants of Shenzhen Science and Technology Peacock Team Project: No. KQTD201703311453160; Basic Research Subject Layout Project of Shenzhen Science and Technology Plan: No. JCYJ20160328144536436; Basic Research Projects of Shenzhen Science and Technology Plan: No. JCYJ 20160429114659119, JCYJ 20170307162947583 and JCYJ 201703071636362.

Conflict of interest

The authors certify that there is no conflict of interest with any individual/organization for the present work.

Author Contributions

Jie Liu, Huailing Wang performed experiments, analyzed data, and review the manuscript, Qinmiao Huang, Xizhuo Sun and Zhendan He designed and supervised the study, and wrote the manuscript, Liteng Yang, Shuqi Qiu, Lin MeiY provided intellectual input and aided in the experimental design. All authors read and approved the final version of the manuscript.

Reference

- [1] Koizumi, W., *Chemotherapy for Advanced Gastric Cancer: Review of Global and Japanese Status*. *Gastrointestinal Cancer Research Gcr*, 2007. **1**(5): p. 197-203.

- [2] Nadaf, A.S., H. Rani, and U.S. Dinesh, *Immuno-Histochemical Assessment of HER2NEU Expression in Gastric Adenocarcinoma in North Karnataka, India*. Asian Pacific Journal of Cancer Prevention Apjcp, 2018. **19**(5): p. 1381-1385.
- [3] Yuan-ZhiZhang, et al., *Clinical phenotype and prevalence of hereditary nonpolyposis colorectal cancer syndrome in Chinese population*. World Journal of Gastroenterology. **11**(10): p. 1481-1488.
- [4] Chang, W.K., et al., *Association between Helicobacter pylori infection and the risk of gastric cancer in the Korean population: prospective case-controlled study*. Journal of Gastroenterology. **36**(12): p. 816-822.
- [5] Lan, Y.-Q., et al., *Combination chemotherapy with paclitaxel and oxaliplatin as first-line treatment in patients with advanced gastric cancer*. Cancer Chemotherapy & Pharmacology, 2018. **81**(1).
- [6] Tokito, T., et al., *Toxicity and efficacy of chemotherapy for non-small cell lung cancer with cavitory lesions*. Respiratory Investigation. **52**(3): p. 184-189.
- [7] Xiu-Min Li, M.D., *Treatment of Asthma and Food Allergy With Herbal Interventions From Traditional Chinese Medicine*. Mount Sinai Journal of Medicine A Journal of Translational & Personalized Medicine, 2011. **78**(5): p. 697-716.
- [8] Yan, X. and L. Jing-Yu, *Chemical Constituents of Sonchus oleraceus L.* Journal of China Pharmaceutical University, 2005.
- [9] Yin, J., *Antioxidant Activity of Flavonoids and Their Glucosides from Sonchus oleraceus L.* Journal of Applied Biological Chemistry, 2008. **51**(2): p. 57-60.
- [10] Miyase, T. and S. FUKUSHIMA, *Studies on sesquiterpene glycosides from Sonchus oleraceus L.* Chemical & Pharmaceutical Bulletin. **35**(7): p. 2869-2874.
- [11] Vilela, F.C., et al., *Evaluation of the antinociceptive activity of extracts of Sonchus oleraceus L. in mice*. **124**(2): p. 0-310.
- [12] Jie, Y., G.J. Kwon, and M.H. Wang, *The antioxidant and cytotoxic activities of Sonchus oleraceus L. extracts*. Nutrition Research & Practice, 2007. **1**(3): p. 189-194.
- [13] Brahmane, R.I., et al., *Partial in vitro and in vivo red scorpion venom neutralization activity of Andrographis paniculata*. Pharmacognosy Research, 2011. **3**(1): p. 44-48.

- [14] Cao, H., et al., *Structural characterization of peptides from <i>Locusta migratoria manilensis</i> (Meyen, 1835) and anti-aging effect in <i>Caenorhabditis elegans</i>*. Rsc Adv. **9**(16): p. 9289-9300.
- [15] Lu, S., et al., *Radiosensitization of clioquinol and zinc in human cancer cell lines*. BMC Cancer, 2018. **18**(1): p. 448.
- [16] Koumtebaye, E., et al., *Antitumor activity of Xiaoaiping injection on human gastric cancer SGC-7901 cells*. Chinese Journal of Natural Medicines. **10**(5): p. 339-346.
- [17] Wei, Z. and Z. Liang, *Comparison between annexin V-FITC/PI and Hoechst33342/PI double stainings in the detection of apoptosis by flow cytometry*. Chinese Journal of Cellular & Molecular Immunology, 2014. **30**(11): p. 1209-1212.
- [18] Cossarizza, A., *A new method for the cytofluorimetric analysis of mitochondrial membrane potential using the J-aggregate forming lipophilic cation 5,5',6,6'-tetrachloro-1,1',3,3'-tetraethylbenzimidazolcar-bocyanin iodide (JC-1)*. Biochem Biophys Res Commun, 1993. **30**(1): p. 40-45.
- [19] Amini, N., et al., *Production and characterization of a polyclonal antibody against an actin peptide*. Iranian Journal of Basic Medical Sciences, 2011. **44**(13): p. 653-660.
- [20] Cao, H., et al., *Structural characterization of peptides from <i>Locusta migratoria manilensis</i> (Meyen, 1835) and anti-aging effect in <i>Caenorhabditis elegans</i>*. RSC Adv. **9**(16): p. 9289-9300.
- [21] Pozzo, C. and C. Barone, *Is There an Optimal Chemotherapy Regimen for the Treatment of Advanced Gastric Cancer That Will Provide a Platform for the Introduction of New Biological Agents?* Oncologist. **13**(7): p. 794-806.
- [22] Wang, X., et al., *Pharmacokinetics screening for multi-components absorbed in the rat plasma after oral administration traditional Chinese medicine formula Yin-Chen-Hao-Tang by ultra performance liquid chromatography-electrospray ionization/quadrupole-time-of-flight mass sp*. Analyst, 2011. **136**.
- [23] Chaube, S.K., et al., *Hydrogen peroxide modulates meiotic cell cycle and induces morphological features characteristic of apoptosis in rat oocytes cultured in vitro*. Apoptosis. **10**(4): p. 863-874.

- [24] Brill, A., et al., *The Role of Apoptosis in Normal and Abnormal Embryonic Development*. Journal of Assisted Reproduction & Genetics. **16**(10): p. 512-519.
- [25] Pommier, Y., Q. Yu, and K.W. Kohn, *NOVEL TARGETS IN THE CELL CYCLE AND CELL CYCLE CHECKPOINTS*. 2002: p. 13-30.
- [26] Lane, M.E., et al., *A Screen for Modifiers of Cyclin E Function in Drosophila melanogaster Identifies Cdk2 Mutations, Revealing the Insignificance of Putative Phosphorylation Sites in Cdk2*. Genetics, 2000. **155**(1): p. 233-44.
- [27] He, G., et al., *Upregulation of p27 and its inhibition of CDK2/cyclin E activity following DNA damage by a novel platinum agent are dependent on the expression of p21*. British Journal of Cancer. **95**(11): p. 1514-1524.
- [28] Morii, M., et al., *Imatinib inhibits inactivation of the ATM/ATR signaling pathway and recovery from adriamycin/doxorubicin-induced DNA damage checkpoint arrest*. Cell Biology International. **39**(8): p. 923-932.
- [29] Gottifredi, V., et al., *p53 down-regulates CHK1 through p21 and the retinoblastoma protein*. 2001. **21**(4): p. 1066-1076.
- [30] Tamara, D., et al., *Involvement of oxidative stress response genes in redox homeostasis, the level of reactive oxygen species, and ageing in Saccharomyces cerevisiae*. Fems Yeast Research, 2005(12): p. 12.
- [31] Kim, H.J., et al., *Preferential elevation of Prx I and Trx expression in lung cancer cells following hypoxia and in human lung cancer tissues*. Cell Biology & Toxicology. **19**(5): p. 285-298.
- [32] Zhang, X.J., et al., *Strophalloside Induces Apoptosis of SGC-7901 Cells through the Mitochondrion-Dependent Caspase-3 Pathway*. Molecules. **20**(4): p. 5714-5728.
- [33] Ji, B.C., et al., *Gallic Acid Induces Apoptosis via Caspase-3 and Mitochondrion-Dependent Pathways in Vitro and Suppresses Lung Xenograft Tumor Growth in Vivo*. J Agric Food Chem. **57**(16): p. 7596-7604.